

(2)

# UMENTATION PAGE

Form Approved
OMB No 0704-0188



| 1. AGENCY USE ONLY (Leave blank) | 2. REPORT DATE | 3. REPORT TYPE AND DATES COVERED |
|---|---|---|
| | | Reprints |

**4. TITLE AND SUBTITLE**

DROPLET SIZING USING THE SHIFRIN INVERSION

**5. FUNDING NUMBERS**

DAAL03-92-G-0122

**6. AUTHOR(S)**

R. Albert and P.V. Farrell



**7. PERFORMING ORGANIZATION NAME(S) AND ADDRESS(ES)**

University of Wisconsin-Madison
Engine Research Center
1500 Johnson Drive
Madison, WI 53706

**8. PERFORMING ORGANIZATION REPORT NUMBER**

**9. SPONSORING/MONITORING AGENCY NAME(S) AND ADDRESS(ES)**

U. S. Army Research Office
P. O. Box 12211
Research Triangle Park, NC 27709-2211

**10. SPONSORING/MONITORING AGENCY REPORT NUMBER**

ARO 30340.2-EG-URI

**11. SUPPLEMENTARY NOTES**

The view, opinions and/or findings contained in this report are those of the author(s) and should not be construed as an official Department of the Army position, policy, or decision, unless so designated by other documentation.

**12a. DISTRIBUTION/AVAILABILITY STATEMENT**

Approved for public release; distribution unlimited.

**12b. DISTRIBUTION CODE**

**13. ABSTRACT** (Maximum 200 words)

A method for measuring droplet size distributions was investigated with an emphasis on limitations related to measurements in real spray environments. The method stores a photographic image of a plane of droplets within a spray and is capable of evaluating particle size distributions within the spray, one small region at a time. The method complements droplet velocity measurements made using Particle Image Velocimetry. In a typical experiment, a plane of the spray was illuminated by a laser light sheet and photographed. After processing, a small laser beam scanned the film and a diffraction pattern was generated for each region illuminated by the small laser. The diffraction pattern was inverted using a Shifrin inversion to solve for the particle size distribution within the illuminated region.

When applied to real particle images for either monodisperse or polydisperse particle distributions, the results of the Shifrin inversion are affected by constraints on the range and quality of the intensity data. Some of these constraints are imposed by hardware limitations and some are imposed by the coherent reconstruction system itself. In this paper we will discuss some of these limitations and indicate one approach which seems to allow for improved inversions using data signal processing.

Experimental data for use with the measurement method was generated using water doped with 2',7' dichlorofluorescein from an atomizer.

**14. SUBJECT TERMS**

Particle sizing, diffraxtion, shifrin inversion

**15. NUMBER OF PAGES**

7

**16. PRICE CODE**

| 17. SECURITY CLASSIFICATION OF REPORT | 18. SECURITY CLASSIFICATION OF THIS PAGE | 19. SECURITY CLASSIFICATION OF ABSTRACT | 20. LIMITATION OF ABSTRACT |
|---|---|---|---|
| UNCLASSIFIED | UNCLASSIFIED | UNCLASSIFIED | UL |

THE AMERICAN SOCIETY OF MECHANICAL ENGINEERS
345 E. 47 St., New York, N.Y. 10017

92-WA/FE-1





# Droplet Sizing Using the Shifrin Inversion

**R. ALBERT and P. V. FARRELL**
Department of Mechanical Engineering
University of Wisconsin-Madison
Madison, Wisconsin 53706

## Abstract

A method for measuring droplet size distributions was investigated with an emphasis on limitations related to measurements in real spray environments. The method stores a photographic image of a plane of droplets within a spray and is capable of evaluating particle size distributions within the spray, one small region at a time. The method compliments droplet velocity measurements made using Particle Image Velocimetry. In a typical experiment, a plane of the spray was illuminated by a laser light sheet and photographed. After processing, a small laser beam scanned the film and a diffraction pattern was generated for each region illuminated by the small laser. The diffraction pattern was inverted using a Shifrin inversion to solve for the particle size distribution within the illuminated region.

When applied to real particle images for either monodisperse or polydisperse particle distributions, the results of the Shifrin inversion are affected by constraints on the range and quality of the intensity data. Some of these constraints are imposed by hardware limitations and some are imposed by the coherent reconstruction system itself. In this paper we will discuss some of these limitations and indicate one approach which seems to allow for improved inversions using data signal processing.

Experimental data for use with the measurement method was generated using water doped with 2',7' dichlorofluorescein from an atomizer.

## Nomenclature

d = particle diameter
$I_\theta$ = intensity at an angle $\theta$ from the optical axis
k = wave number, $2\pi/\lambda$
n(x) = particle distribution function
x = particle size parameter, $\pi d/\lambda$
$x_1$ = limit of integration for size parameter in eqn (1)
$x_2$ = limit of integration for size parameter in eqn (1)
y = particle parameter, $x\theta$
z = distance from particle image to image plane for interrogation
$\lambda$ = wavelength of light
$\theta$ = angle from optical axis

## Introduction

A significant number of two-phase flow problems are of short duration, or exhibit important transient characteristics upon starting or stopping, or are in a turbulent flow field. Any of these conditions renders many of the details of the flow unsteady. Measurement of the spatially resolved transient behavior of the flow field may provide better understanding of two-phase flow behavior

Current experimental techniques for measuring particle size and velocity have been carefully developed and appear to be mature techniques. These include Fraunhofer diffraction measurements (Swithenbank, et al., 1976 and Yule, et al., 1982), interferometric intensity type measurements (Farmer, 1972 and Bachalo, 1980), and phase Doppler type measurements (Bachalo and Houser, 1984). Comparisons of these techniques are given by Jackson and Samuelson (1987) and Dodge, et al. (1987) and recent summaries are given by Hirleman, et al. (1990).

These techniques make measurements at a single point or measurements averaged over some small area of the flow. They can make a series of measurements at a given location over time. For transient flows, particularly ones with significant turbulence and other stochastic characteristics, a collection of single point time records spanning some spatial region of interest is difficult to interpret. The various spatial locations would be sampled at different discrete times, for what may amount to different flow conditions. For many transient multi phase flow applications, measurements which span a spatial area or volume at a series of discrete times may be of greater utility in developing an understanding of the flow as well as for development and refinement of flow models.

## Measurement Technique Background

The basis of the method for measuring particle size and velocity is similar to the developing technique of particle image velocimetry (PIV). A brief review of the concepts necessary for this measurement technique will be presented

Particle image velocimetry has been described in a complete review by Adrian (1991). The general technique of PIV involves a multiple exposure photograph of a flow containing particles or droplets. A photographic image of the particles is obtained for a

Presented at the [illegible] Annual Meeting
November 8-13, 1992—Anaheim, CA

plane of particles which has dimensions of the height of an illuminating laser sheet, the width of the image plane, and the thickness of the laser sheet. Typical dimensions are 3 cm high by 5 cm wide by 200 μm thick. The light source is usually controlled to allow two exposures of the particle field to be recorded on the film. The time between the exposures is controlled and is presumed known. Particle velocity can be obtained by measuring the magnitude and direction of the displacement of a particle between exposures.

After development, the film is illuminated with an unexpanded laser beam. Sequential illumination of portions of the film provides information regarding particle displacement in the region illuminated. Each particle image generates a diffraction pattern in the far field (far from the film). The combination of the many diffraction patterns from many particle images illuminated by the laser beam produces an interference pattern, known as Young's fringes. The low frequency modulation of the fringe pattern is known as the diffraction halo.

Particle size information is available from the shape of the diffraction halo which modulates the Young's fringe pattern. Since the Fourier transform or far-field diffraction operator is linear, the effects of many particles may be interpreted through superposition. The diffraction halo is the same diffraction pattern for near forward scattering from particles which is observed for diffraction based particle sizing techniques (Swithenbank, et al., 1976).

Inversion of the scattered intensity data, minus the higher frequency Young's fringe data, can provide a particle size distribution of the ensemble of particle images which appear within the interrogating laser beam. It may be noted that in dilute regions of a spray, the small sample volume interrogated may cover a few droplets, not enough to be reliably predicted with a continuous size distribution. Thus in inverting the diffraction halo intensity pattern to recover a particle size distribution, it is unlikely that an *a priori* selected distribution function will be successful.

For particle size measurements a TV camera is used to capture the diffraction pattern and Young's fringe pattern at the back focal plane of the lens, as shown in Fig. 1a, along with a typical photographic set-up in Figs. 1b and 1c. The use of a TV camera as a detector has the advantage of simultaneous use for PIV applications and selectivity of geometry of data collection. With the camera, information in the intensity profile can be collected at different sector sizes and at different angles within each sector. A disadvantage of using a TV camera is the limited dynamic range of the attached frame grabber, which in our case is 8 bits for each pixel. In our analysis some high intensity information in the small diffraction angle region was sacrificed (overexposed or saturated) to pick up information at higher scattering angles.

The intensity pattern captured by the TV camera can be sampled in a variety of ways, using line scans of the image in selected directions, integrating rings at specified radii to imitate ring detectors (Kouzalis, et al, 1988), or integrating over selected sectors of rings. In the experiments discussed here, little difference was seen in the results for line scans and sectors integrated over as much as $45^{o}$. Since line scans are much faster, these are used for the results.

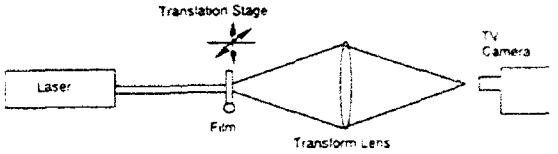


Figure 1a: Interrogation system for PIV and particle sizing method

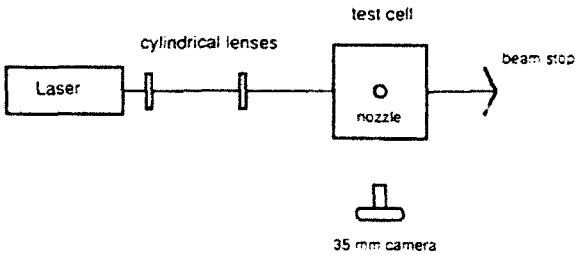


Figure 1b: Experimental arrangement for spray photography, plan view

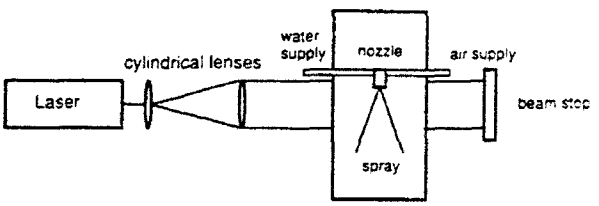


Figure 1c: Experimental arrangement for spray photography, elevation

The diffraction halo due to particle scattering is the low frequency portion of the Young's fringe pattern, which is given by the Airy formula

$$I_\theta = \frac{1}{k^2\theta^2 z^2}\int_{x_1}^{x_2} J_1^2(y)x^2 n(x)dx \qquad (1)$$

where θ is an angle measured from the center of the diffraction pattern, $I_\theta$ is the normalized scattered intensity at an angle θ, $k = 2\pi/\lambda$, λ is the wavelength of light, z is the distance from the diffracting object to the viewing plane, x is the particle size parameter $x = \pi d/\lambda$, $x_1$ and $x_2$ are limits on the expected particle size parameter, n(x) is the particle size distribution, $\theta \approx \sin\theta$, $y = x\theta$, and $J_1$ is a Bessel function of the first kind of order unity. For some distributions n(x) may be assumed to vanish at $x_1$ and $x_2$, giving

$$I_\theta = \frac{1}{k^2\theta^2 z^2}\int_0^\infty J_1^2(y)x^2 n(x)dx \qquad (2)$$

Equation (2) may be considered a first-kind Fredholm integral equation. An inversion producing n(x), known as a Shifrin inversion, is possible (Fymat and Mease, 1978) resulting in

$$n(x) = -\frac{2\pi k^2 z^2}{x^2}\int_0^\infty J_1(y)Y_1(y)y\frac{d(\theta^3 I_\theta)}{d\theta}d\theta \qquad (3)$$

where $Y_1$ is a Bessel function of the second kind of order 1.

This type of data inversion allows flexibility in the type of particle size distribution acquired, since no distribution is assumed. A major disadvantage of this integral inversion scheme is that the measured data, $I_\theta$, must be differentiated. Alternative inversion methods using the Shifrin inversion in other forms (Fymat and Mease, 1978 and Coston and George, 1991) and the use of other inversion schemes (Hirleman, 1991) have been suggested. Some of these inversions are aimed primarily at ring detector geometry, but others which may prove useful in this application have not yet been implemented. It should be noted that the result of the calculation from Eqn. 3 is a relative particle size distribution, and actual particle flux or mass flux of particles is not a result of Eqn. 3. Estimates of total particle flux for diffraction based methods are usually made by measurement of the attenuation of the interrogating laser beam relative to a correlation for extinction as a function of flux.

The technique outlined has been tested on modeled and experimental single apertures, a variety of modeled polydisperse distributions, a fixed calibration reticule, and a monodisperse droplet stream (Farrell, 1991). The results of this previous work indicated that the inversion scheme worked well for both monodisperse and polydisperse size distributions using modeled intensity data. Using experimental data from single apertures, the method was able to accurately measure monodisperse distributions. Using a reticule with a Rosin-Rammler distribution of plated spots, the method was able to accurately measure the distribution. An example of the size distribution measured for the Rosin-Rammler distribution of the spots on a reticule is shown in Fig. 2. The results for the distribution agree fairly well with the "given" distribution for the images. In the previous work, the method had not been extensively tested in spray fields subject to laser speckle and other noise sources.

When the experimental method described was applied to a spray, several problems were observed which were not clearly evident in the single aperture and polydisperse reticule evaluations. For a typical application, a large spray field is photographed, either with single or double exposure, and interrogated on a scale of about 0.5 mm. For many regions of a spray, this geometric scale will include a small number of droplets. In these regions, system performance for monodisperse or multi mode size distributions is important.

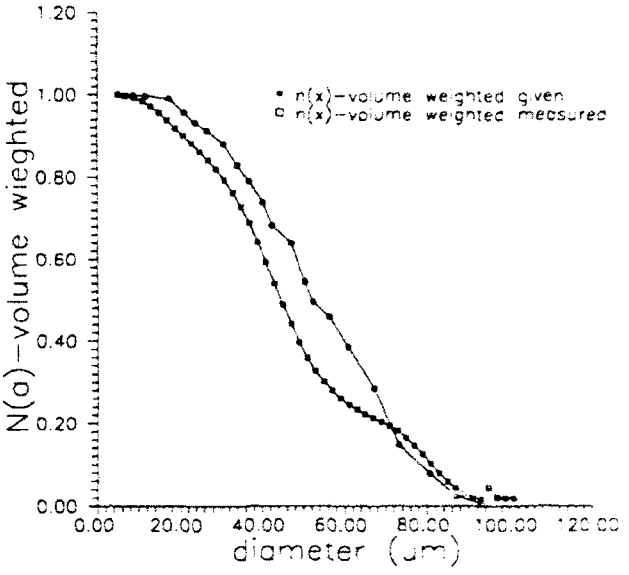


Figure 2. Experimental distribution profile for Rosin-Rammler distribution, compared with data supplied with reticule

**Particle Sizing Method Improvements**

The particle sizing method may be characterized using calculated intensity distributions for monodisperse or polydisperse particle distributions. Experimental monodisperse and polydisperse distributions can also be evaluated, although quantitative comparison for polydisperse distributions is difficult since the actual distribution is rarely known.

A calculated intensity profile for a 50 µm particle is shown in Fig. 3. This figure shows a slice through the cross section of the Airy pattern described in Eqn. (2). The numerical intensity pattern has been truncated in the figure to expand the intensity scale at the lower intensity values, but the complete intensity profile is used in the inversion calculations. Using the Shifrin inversion, the area weighted number distribution, $x^2n(x)$, calculated using the Shifrin inversion is shown in Fig. 4. A 50 µm aperture intensity profile was measured experimentally, and the area weighted size distribution was calculated. These profiles are also shown in Fig. 3 and Fig. 4. Note that the experimental intensity profile in Fig. 3 has saturated the detector (TV camera) for the first two peaks. As indicated in Fig. 4, the actual aperture diameter was slightly larger than 50 µm. It was measured to be about 53 µm.

In comparison to the numerical intensity distribution in Figs. 3 and 4, the experimental distribution shows greater noise and a limited range of θ over which the intensity signal is above the noise floor. As a result, the integration in the Shifrin inversion is carried out over a smaller range of significant θ values, and the resulting distribution in Fig. 4 shows broader peaks and some "ringing" near the 50 µm peak. For this particular experiment, the noise in the intensity profile is primarily background optical noise (e.g. laser speckle) so camera and digitizer noise are not the major contributors. If the ripple in the distribution in Fig. 4 is considered to be random noise, an RMS noise value can be calculated for each of the profiles in Fig. 4. The numerical profile has an RMS noise figure of 0.761% of the peak signal, while the experimental profile

has an RMS noise figure of 3.465% of the peak signal. Clearly the noise in these distributions is not random, and the RMS noise does not accurately characterize the ability to identify distribution peaks, but this type of calculation gives a numerical comparison of the ripple of the distribution function.

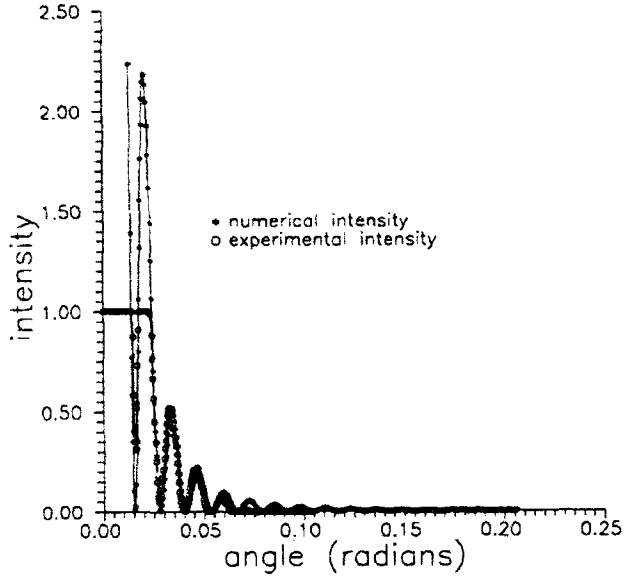


Figure 3: Intensity profiles for numerical and experimental data

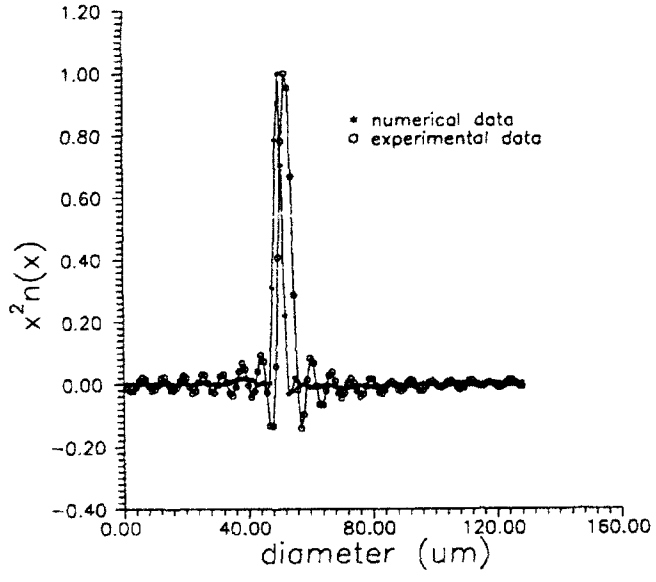


Figure 4: Comparison of area weighted size distributions for numerical and experimental data

Reducing the range of θ over which the numerical intensity profile is sampled or has significant content produces characteristics similar to the experimental aperture results, indicating that the limitation to relatively small θ values has a significant impact on the calculated size distribution and the distribution pattern. The effect of reduced total angle over which data can be collected is shown in Figs. 5 and 6 in which numerically generated intensity profiles for a 50 μm particle have been truncated to smaller total sampling angles. In Fig. 5, the number of sample values is changed while the Δθ is held constant, and in Fig. 6, the number of sample values is held constant and Δθ is allowed to vary. In either case, the overall angle for sampling, $\theta_{max}$, has a significant effect on the size distribution pattern. The RMS noise in the size distribution, calculated as for Fig. 4, ranges from .76% to 11.44% in Fig. 5 and from .76% to 11.29% in Fig. 6.

When using intensity profiles for monodisperse distributions, the required range of θ is significantly larger than for the polydisperse case. This increase in required effective sampling angle for monodisperse distributions has been previously noted by Fymat and Mease (1978). In the current measurement method, a large portion of the particle image photograph lies in a region where a small number of particles will be sampled by the unexpanded laser beam at any one time. Thus, performance on monodisperse distributions or small numbers of particle sizes is important in the overall performance of the system.

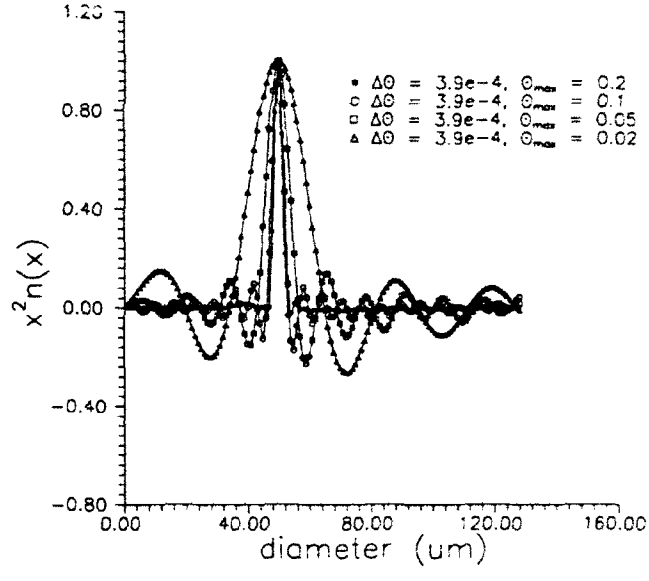


Figure 5: Numerical data with variation of $\theta_{max}$, Δθ constant

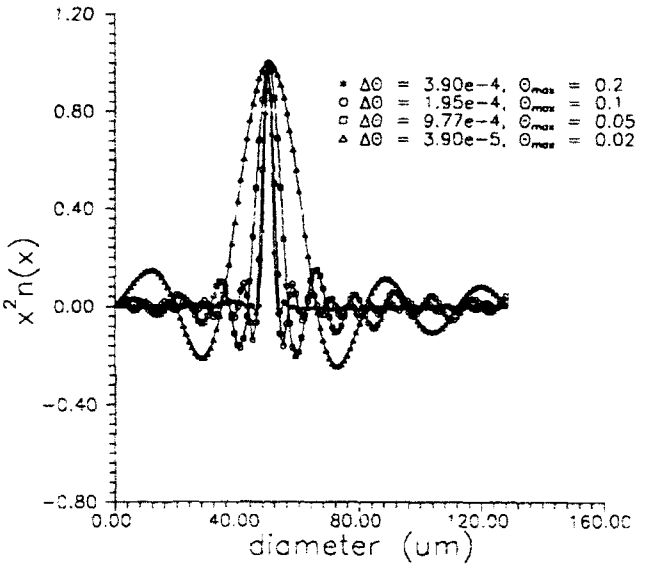


Figure 6: Numerical data with variation of $\theta_{max}$, $N_\theta$ constant

Several approaches to "extrapolate" the measured data to larger θ values for monodisperse distributions have been tried, and one shows some promise. Theoretical particle size distributions produce intensity distributions which are essentially integrals of Bessel functions (Eqn. 1). A part of the kernel of the integral used in the Shifrin inversion is the term

$$\frac{d(\theta^3 I_\theta)}{d\theta} \qquad (4)$$

which for numerically generated monodisperse size distributions is essentially a cosine wave. In order to extrapolate the range of θ over which this term is available (non-zero and not dominated by noise), the existing portion of the kernel is treated in a manner similar to those used for calculations of super resolution in optics. The kernel cited in Eqn. 4, as a function of θ, is Fourier transformed using an FFT routine. In the Fourier plane, the available frequency values may be used to generate more values by interpolating between calculated frequency values. In our implementation, using a trapezoidal rule, this technique effectively doubles the number of frequency samples. Upon inverse Fourier transformation, the reduction of Δf by a factor of 2 leads to an increase in the total θ range of the function by a factor of 2. This method assumes that all significant frequency content of the kernel is already present in the original data. The result represents extrapolated data which is consistent with the original values in terms of frequency content. In an effort to filter the high frequency noise typically present on experimental signals, we also window the frequency spectrum before inverse transformation using a Blackman-Harris type window. After this extrapolation procedure, the newly lengthened kernel is used in the Shifrin inversion to determine the particle size distribution.

This technique has almost no effect on numerically derived intensity distributions, since typically any range of θ values may be selected when the intensity distribution is generated. For monodisperse experimental data, the extrapolation of the data has an effect, giving larger peak values for the area weighted size distribution, and less ripple in the size distribution. An example of the results of this type of data extrapolation is shown in Fig. 7. This figure shows the results of two inversions from an experimentally derived intensity distribution for a nominally 50 μm aperture. One of the inversions, labeled with the stars, is the inversion from the original data set, without extrapolation or filtering. The second profile, labeled with the circles, is from the transformed, interpolated, filtered, and inverse transformed data. The two profiles are clearly similar, but the extrapolated one exhibits a slightly wider profile at the 50 μm particle size and significantly reduced ripple elsewhere. Using the RMS noise as an estimate of the ripple in the size distribution, the "original data" in Fig. 7 has an RMS noise of 3.46% and the "extrapolated data" has an RMS noise of 1.82%.

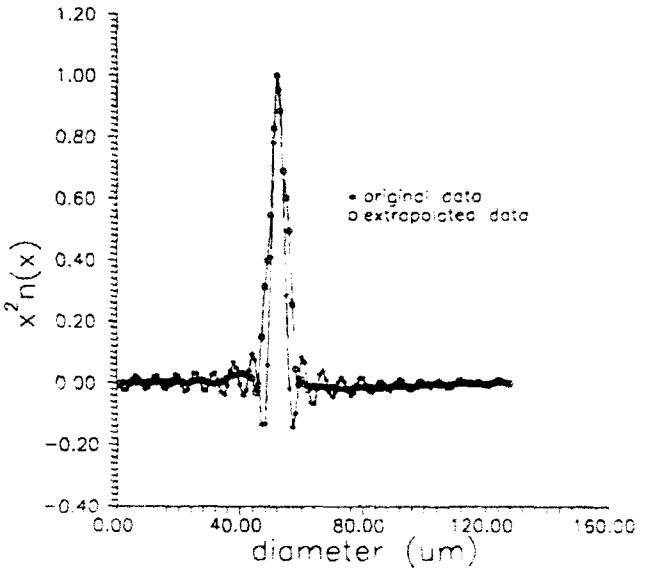


Figure 7. Comparison of original experimental data with extrapolated data

**Spray System**

Experimental results from a water spray are shown to indicate how the method performs on an actual spray. Since the size distribution in the regions interrogated by the laser is not known, only qualitative evaluations of the system performance is possible under these conditions.

A spray chamber was designed and built of acrylic with three windows to serve as entry and exit points for the laser sheet and as a window for photography. A Spraying Systems nozzle, which was an external mix, round spray, full cone atomizer (1/4J, 64SS air cap, 1650SS fluid cap, with No. 12810 liquid shut off needle) was used. The chamber allowed both horizontal and vertical nozzle translation relative to the laser sheet location. The air was supplied under pressure from the house supply directly to the nozzle and the liquid was siphon fed from a 500 ml beaker.

A doubled Nd:Yag laser supplied illumination of the spray by providing high intensity light in a pulse duration of about 6 ns operating at a wavelength of 532 nm. Two cylindrical lenses shaped the laser beam. The light was expanded by the first lens to a height of 40 mm at the test chamber. The second cylindrical lens

decreased the 7 mm width of the beam to about 1 mm at the location of the spray. A sketch of the system is shown in Figs. 1b and 1c.

A 35 mm camera with a 105 mm focal length lens with a focusing tube was used to take the photographs of the spray. A magnification of 1:1 was chosen for simplicity. The imaged droplets at 90° scatter appeared as a front and a back arc, or in some cases as a disk. For the analysis scheme, filled-in images were needed. To solve this problem 2',7' Dichlorofluorescein was used. to dope the water spray to provide fluorescence from the 532 nm source. The sprayed solution contained 1 g of the chemical for every 200 ml of water and the remaining solids were filtered with Whatman #1 filter paper. A hydrometer determined the specific gravity of the solution to be the same as that of water. The Dichlorofluorescein is listed as a low hazard material with usual industrial handling. A wet vacuum, equipped with a foam filter sleeve, was connected to the bottom of the spray chamber and the exhaust was vented directly into the outgoing building exhaust.

The parameters which could be varied during the experiment were the supply air pressure (which correspondingly altered the liquid flow rate) and the horizontal and vertical nozzle positions. For this paper, one setting of these values was used, since the emphasis was on the inversion scheme.

In the region of interrogation, the droplet images on the film typically range from 15 to 70 μm, and are relatively well dispersed. Original and extrapolated data results are plotted in Figs. 8 and 9 for samples taken at two different locations of the water spray from the air-assisted atomizer. These locations were chosen arbitrarily to indicate the general types of particle distributions available, and are not intended to comprehensively describe the spray itself. In each figure, a plot of the size distribution from unextrapolated data is shown in comparison with the distribution using extrapolated and filtered data. Note that for these figures the particle size distribution is plotted, not the area weighted distribution. The regions sampled have a few to several particles within the region, and the size distributions should reflect that kind of multi mode character. The extrapolated data appear to have somewhat reduced oscillation in the n(x) profiles with respect to the unextrapolated versions. Each sampled region has only a few particles in it, so each peak in the size distribution may be interpreted as one or more particles at that size.

The size distributions shown in Figs. 8 and 9 are not as well defined as those for the single apertures, in Fig. 7, for example. Figure 8 shows a large peak at about 20 μm and smaller peaks at about 30 μm and 70 μm, all of which are likely to represent single particles of these respective sizes. The remainder of the distribution in Fig. 8 shows remnants of the ripple seen on other examples, but looking at the "extrapolated" results, the remaining peaks do not appear to rise above the background ripple. Using the RMS noise calculation used in Fig. 7 comparisons, the extrapolated size distribution for Fig. 8 exhibits an RMS noise value of 3.95% of the peak value, while the original data has an RMS noise figure of 5.66% of the peak value. In Fig. 9, large values of the distribution function are evident at about 15 μm and again at about 25 μm, 39 μm, and 55 μm. Each of these peaks likely represents a single droplet of that size. The remainder of the distribution, at larger droplet sizes, appears to be primarily background ripple. The RMS noise figure for the extrapolated data in Fig. 9 is 11.5% of the peak value, while the original data has a noise figure of 16.5% of the peak value. In both of these cases, the use of the extrapolation scheme appears to reduce the magnitude of the background ripple due to limited angular data range, making the distribution peaks more readily identifiable.

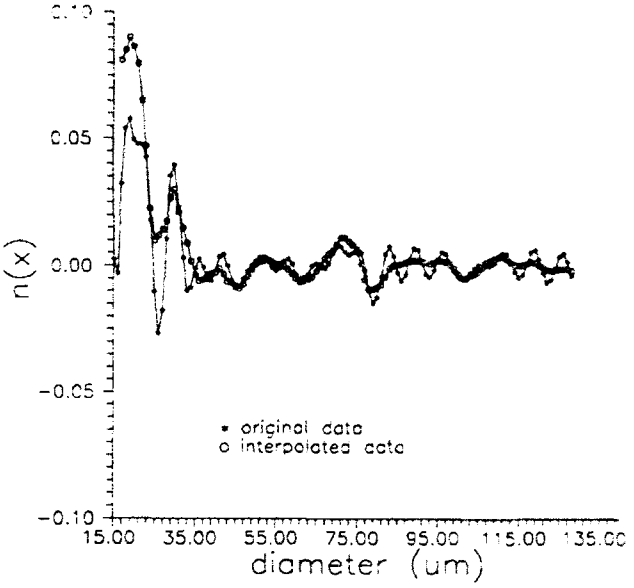


Figure 8: Sample size distribution from spray

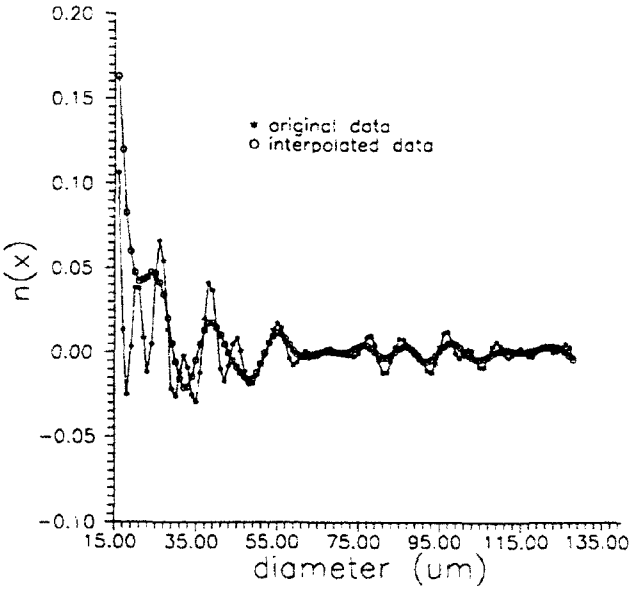


Figure 9: Sample size distribution from spray

**Conclusions**

This paper discusses a technique for droplet sizing in a polydisperse atomizer spray. The major focus of the paper is to indicate how the current inversion scheme's level of performance is affected by limited data collection range caused by experimental noise. A method is proposed for extrapolation of the data to larger

sampling angles through interpolation in the frequency domain. Some examples of the performance of the system are presented for single apertures and for portions of a spray. On single aperture data, the "noise" in the size distribution interpreted as random RMS noise, decreases by a factor of almost 2, compared to a similar "noise" measurement on unextrapolated data. On experimental data from a water spray, size distributions are qualitatively improved and size peaks made more identifiable. The reduction in noise, using the calculated RMS noise as a figure of merit, is smaller for the spray data than for the apertures, with typical reductions of about 1/3.

**Acknowledgments**

This work was supported in part by a grant from the National Science Foundation CTS-9106568, and by the designation of the Engine Research Center as a DOD Center of Excellence for Propulsion.

**References**

Adrian, R. J. 1991, "Particle imaging techniques for experimental fluid mechanics," in **Ann. Rev. Fluid Mech. 1991**, p. 261.

Bachalo, W. D., 1980, "Method for measuring the size and velocity of spheres by dual-beam light-scatter interferometry," **Applied Optics 19**, p. 363.

Bachalo, W. D. and Houser, M. J., 1984, "Phase/Doppler spray analyzer for simultaneous measurements of drop size and velocity," **Opt. Eng. 23**, p. 583.

Coston, S. D. and George, N., 1991, "Particle sizing by inversion of the optical transform pattern," **Applied Optics 30**, p. 4785.

Dodge, L. G., Rhodes, D. J., and Reitz, R. D., 1987, "Drop-size measurements techniques for sprays: comparison of Malvern laser-diffraction and Aerometrics phase/Doppler," **Applied Optics 26**, p. 2144.

Farmer, W. M., 1972, "Measurement of particle size, number density, and velocity using a laser interferometer," **Applied Optics 11**, p. 2603.

Farrell, P. V. , 1991,"Particle sizing using a two-dimensional image," SAE Paper 910725.

Fymat, A. L. and Mease, K. D., 1978, "Reconstructing the size distribution of spherical particles from angular forward scattering data," in **Remote Sensing of the Atmosphere, Inversion Methods and Applications**, A. L. Fymat and V. E. Zueu, eds. Elsevier.

Hirleman, E. D., 1991, "General solution to the inverse near-forward scattering particle-sizing problem in multiple-scattering environments," **Applied Optics 30**, p. 4832.

Hirleman, E. D., Bachelo, W. D., and Felton, P. G., 1990, **Liquid Particle Size Measurement Techniques: 2nd Volume**, ASTM STP 1083.

Jackson, T. A. and Samuelson, G. S., 1987, "Droplet sizing interferometry: a comparison of the visibility and phase/Doppler techniques," **Applied Optics 26**, p. 2137.

Kouzelis, D., Candel, S. M., Esposito, E., and Zikikout, S., 1988, "Particle sizing by laser light diffraction: improvements in optics and algorithms," in **Optical Particle Sizing**, G. Gousbet and G. Grehan, eds. Plenum.

Swithenbank, J., Beer, J. M., Taylor, D. S., Abbot, D., and McCreath, G. C., 1976, "A laser diagnostic technique for the measurement of droplet and particle size distribution," in Experimental Diagnostics in Gas Phase Combustion, AIAA vol 53, **Progress in Astronautics and Aeronautics**, B. T. Zinn, Ed.

Yule, A. J., Seng, C., Felton, P. G., Ungut, A., and Chigier, N. A., 1982, "A study of vaporizing fuel sprays by laser techniques," **Comb. and Flame 44**, p.71